Journal of the Korean Ceramic Society
Vol. 54, No. 3, pp. 235~242, 2017.

https://doi.org/10.4191/kcers.2017.54.3.08

Experiment and Prediction of Nonlinear Behavior at High Temperatures of Ferroelectric Ceramics Switched by Electric Field at Room Temperature

Dae Won Ji and Sang-Joo Kim†

Department of Mechanical and Information Engineering, University of Seoul, Seoul 02504, Korea

(Received April 10, 2017; Revised May 11, 2017; Accepted May 11, 2017)

ABSTRACT

Changes in polarization and thermal expansion coefficients during temperature increase of a poled lead zirconate titanate (PZT) cube specimen switched by an electric field at room temperature are measured. The measured data are analyzed to construct governing differential equations for polarization and strain changes. By solving the differential equations, an experimental formula for the high temperature behavior of ferroelectric materials is obtained. It is found that the predictions by the formula are in good agreement with measures. From the viewpoint of macroscopic remnant state variables, it appears that the processes of electric field-induced switching at different temperatures are identical and independent of temperature between 20°C and 110°C.

Key words : Ferroelectric, Temperature, Switching, Remnant, Empirical formula

1. Introduction

Piezoelectric ceramic materials are widely used in various fields as sensors, actuators, and memory devices. The researches on the development and applications of piezoelectric elements and systems continue to be actively carried out. Nonetheless, unpredicted and unnecessary domain switching and changes in the internal structure of the piezoelectric elements and systems have frequently been reported to occur during usage, due to an excessive concentration of electric field or stress, and a resulting rapid rise in temperature. Changes in the microscopic internal structure caused by such switching can lead to changes in the macroscopic properties of the piezoelectric material, and unpredictable nonlinear behavior. This can degrade the level of performance intended in the initial design.

Recently, studies were conducted to develop a model for predicting ferroelectric ceramic nonlinear behavior.[1,2] However, most of the research was limited to modeling the behavior at constant room temperature, so there is still a need for expanded research on the behavior at high temperatures. Prior to developing a constitutive model, experimental data on changes in the behavior of remnant state variables and material property changes caused by changing temperatures, need to be acquired and analyzed.

Previous research on the modeling and behavior changes due to temperature variations include the following studies. Grunbichler *et al.*[3] used a developed constitutive model for finite element analysis to understand the nonlinear behavior of piezoelectric materials caused by the stress, electric field, and temperature changes in a multistack piezoelectric actuator. Kungl *et al.*[4] experimentally investigated the effect of temperature on poling strain when an electric field was applied to the piezoelectric material, and they also studied the temperature dependence of the remnant strain. Rauls *et al.*[5] measured the hysteresis curves of PLZT ferroelectric materials, and Senousy *et al.*[6] focused on the effect of the heat generated by the multistack piezoelectric actuator on the changes in the piezoelectric material properties, and performed a numerical analysis for the behavior of piezoelectric materias at high temperature, assuming a 2 stage 90-degree domain switching. Ji and Kim[7] measured the hysteresis curve due to the electric field under various electric field loading rates and temperatures, and the measured data were used to predict the strain behavior. Kim and Kim[8] measured the changes in remnant polarization and transverse remnant strain during temperature increase after an electric field was applied to a PZT wafer at room temperature. Ji and Kim[9] measured the longitudinal and transverse strains of a rectangular PZT ceramic during temperature increase after electric field-induced switching at room temperature and measured the thermal expansion and pyroelectric coefficients. Also, Ji and Kim[10] applied compressive stress at room temperature followed by temperature increase and obtained the changes in the pyroelectric and thermal expansion coefficients. Weber *et al.*[11] measured and analyzed the nonlinear behavior of ferroelectric materials caused by compressive stress at high temperatures.

In this study, to measure the remnant polarization and remnant strains, an electric field was applied to a poled ferroelectric PZT specimen at room temperature in a direction

†Corresponding author : Sang-Joo Kim
E-mail : sangjookim@gmail.com
Tel : +82-2-6490-2387 Fax : +82-2-6490-2384

opposite to the polarization, while increasing the temperature after switching and removing the electric field. Using the method reported by Ji and Kim,[12] an empirical formula for the variations in polarization and strains was derived utilizing the measured data. The calculation values obtained through the derived empirical formula were compared with the experimental values and it was found that the switching process due to the electric field at different temperatures was equivalent from the perspective of macroscopic state variables.

2. Experimental Procedure

A cube PZT specimen with 10 mm sides was used in the experiment. Its density was 7400 kg·m^{-3} and the specimen was manufactured by a company in the UK (PZT5H1, Morgan Technical Ceramics, UK). The specimen was originally poled in the negative x_3 direction(the thickness direction) and switching occurred when the electric field was loaded in the positive x_3 direction at the reference temperature of 20°C. A change in the polarization density occurred when an electric field of 2 MVm^{-1} sinusoidal wave was 0.52 Cm^{-2} so the range of the reference remnant polarization density P_3^{R0} for the specimen was –0.26 Cm^{-2} to +0.26 Cm^{-2} at 20°C.

In this study, electric fields of varying magnitude were applied a total of 14 times so that the magnitudes of reference remnant polarization were distributed at 0.04 Cm^{-2} intervals. The magnitudes of the applied electric field were 0, 0.520, 0.610, 0.649, 0.655, 0.660, 0.665, 0.671, 0.677, 0.684, 0.692, 0.726, and 0.880 MVm^{-1} and the derived reference remnant polarizations P_3^{R0} were –0.256, –0.214, –0.171, –0.135, –0.094, –0.051, –0.018, +0.025, +0.056, +0.094, +0.136, +0.177, +0.221, and +0.262 Cm^{-2}, respectively.

In particular, after reaching P_3^{R0} by an electric field, the leakage current was measured for 5,000 seconds at the reference temperature. Then, after stabilizing the internal structure of the specimen, the temperature of the specimen and an invar specimen (Product No. 318-0285-3, Danyang, China) was increased to 110°C. The rate of temperature increase was 1.2°Cmin^{-1}.

While the temperature increased, the remnant polarization P_3^R was measured and the thermal power changes $\varepsilon_{G/R}$ and $\varepsilon_{G/S}$ were measured for the invar and ceramic specimens using strain gauges. Here, the thermal power variation represents the change in the output value of the strain gauge as the temperature rises. Afterwards, the coefficients of longitudinal and transverse thermal expansion α_3 and α_1, respectively, were calculated using the thermal expansion coefficient of the invar specimen α_R.

The polarization density was measured indirectly using the Sawyer-Tower circuit, and a Keithley 6514 was used to measure the voltage across the capacitor connected serially with the specimen. Changes in the thermal power were measured using strain gauges (WA-03-062TT-350, VISHAY, Germany) attached to the side of the specimens, which could be used in the temperature range from –75°C to 205°C.

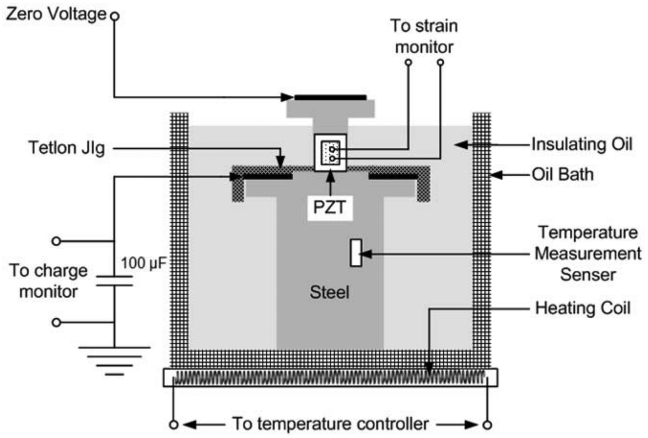

Fig. 1. Schematic experimental setup to measure electric displacement of a poled PZT cube specimen under electric field at room and high temperatures.

The specimen temperature was controlled by placing it in a container (2408 PID controller, EUROTHERM, UK) shown in Fig. 1 with insulating oil (MICTRANS Class1-No2, MICHANG OIL IND. CO., Pusan, Korea) and heating the coil underneath the container. A Teflon jig with a square hole in the center was used as an insulating material between the lower portion of the specimen with high voltage and the grounded top part of the specimen.

All data were collected at 100 Hz through a DAQ unit (PCI 6221, National Instruments, TX, USA) and processed using the LabView program. The specifications of the specimen provided by the manufacturer were as follows. The specimen has a Curie temperature of 200°C, coupling factor of k_p = 0.60, piezoelectric coefficients of d_{31} = –250 × 10^{-12} mV^{-1} and d_{33} = 620 × 10^{-12} mV^{-1}, and elastic compliance coefficient of s_{33} = 21.9 × 10^{-12} m^{2}N^{-1} and s_{11} = 17.7 × 10^{-12} m^{2}N^{-1}. Here, the subscript 3 refers to the polarization direction of the specimen and subscript 1 refers to the direction transverse to the polarization.

3. Result and Discussion

3.1. Changes in Remnant Polarization and Pyroelectric Coefficient During Temperature Increase

Electric fields of various magnitudes were applied to a PZT specimen, which had been poled in the specimen thickness direction. The electric fields were applied in the direction opposite to the polarization at the reference temperature of 20°C. Switching occurred due to the application of the electric field. After reaching a specific reference remnant polarization density, the electric field was removed and the temperature was increased from 20°C to 110°C.

Changes in the ceramic specimen remnant polarization P_3^R were measured during the temperature increase. Fig. 2(a) shows the measured remnant polarization changes that occurred during the temperature increase. Among the 14 reference remnant polarizations, the polarization behaviors

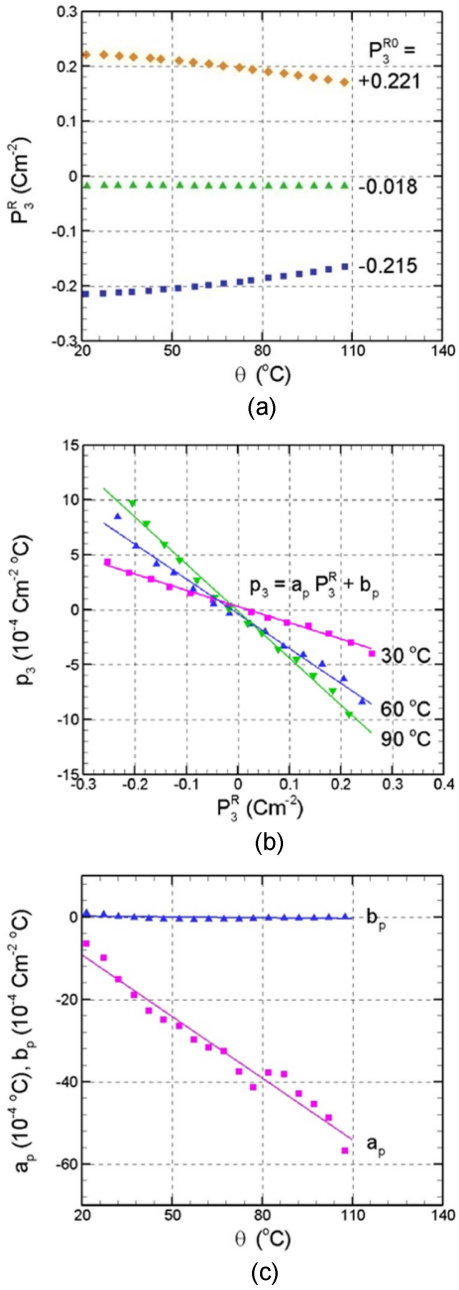

Fig. 2. Measured polarization and construction of an empirical formula for pyroelectric coefficient p_3 during temperature rise at different values of reference remnant polarization P_3^{R0}, obtained by application of electric field at reference temperature of 20°C, (a) P_3^{R0} vs. θ at P_3^{R0} = –0.215, –0.018 and +0.221 Cm^{-2}, (b) p_3 vs. P_3^R at θ = 30°C, 60°C and 90°C, (c) slopes a_P and intercepts b_P of the fitting straight lines in (b) vs. θ.

for the 3 cases of –0.215, –0.018, and +0.221 Cm^{-2} are shown. From the figure, it can be observed that when the temperature increases, the remnant polarization increases when P_3^{R0} is negative, while it decreases when P_3^{R0} is positive. A decrease in the magnitude of remnant polarization can be observed for both cases when the temperature is increased.

When the remnant polarization is near 0, or equivalently, when P_3^{R0} = –0.018 Cm^{-2} in the figure, the magnitude of the polarization is almost constant.

The change in remnant polarization due to temperature is called the pyroelectric coefficient, and it is represented with p_3. In this study, rather than assuming that the pyroelectric coefficient was constant throughout the temperature range from 20°C to 110°C, the pyroelectric coefficient was obtained for every 5°C interval. Fig. 2(a) shows the change in pyroelectric coefficient with the remnant polarization at constant temperatures, in the temperature range from 20°C to 110°C. Fig. 2(b) shows the pyroelectric coefficients obtained for the temperatures of 30, 60, and 90°C based on the remnant polarization. It can be observed that the pyroelectric coefficient data for constant temperatures can be fitted with single lines. Equation (1) below shows the expression for the line.

$$p_3 = a_P P_3^R + b_P, \tag{1}$$

Here, a_P is the slope of the line shown in Fig. 2(b) and b_P is the value of the fitting line value when the reference remnant polarization is 0. The distribution of the values of a_P and b_P for the entire range of 20°C to 110°C is shown in Fig. 2(c). Interestingly, a_P and b_P can also be expressed as straight lines over the temperature. The following equations express the lines.

$$\begin{aligned} a_P &= a_{P\theta}\theta + a_{P0}, \\ b_P &= b_{P\theta}\theta + b_{P0}, \end{aligned} \tag{2}$$

Here, $a_{P\theta}$ and $b_{P\theta}$ are the slopes of the lines shown in Fig. 2(c), and a_{P0} and b_{P0} are the intercept values of the lines at the vertical axis. Substituting Eq. (2) into Eq. (1) results in Eq. (3) below.

$$p_3 = (a_{P\theta}\theta + a_{P0})P_3^R + (b_{P\theta}\theta + b_{P0}). \tag{3}$$

Using Eq. (3), the pyroelectric coefficient p_3 can be calculated when temperature θ and remnant polarization P_3^R are given.

3.2. Changes in Thermal Expansion Coefficient and Remnant Strains During Temperature Increase

In this study, to compensate for the error in measured strain due to high temperature, the thermal expansion coefficient was measured first for the specimen using the invar specimen, then integrated to obtain the strain value, rather than using the temperature compensation curve provided by the manufacturer. In order to obtain the coefficient of thermal expansion of the specimen, the same strain gauges were attached to the ceramic and invar specimens, and then the thermal power from each gauge was measured as the temperature was increased. The equation for calculating the thermal expansion coefficient in the VISHAY manual[13] is as follows.

$$\alpha_S - \alpha_R = \frac{\varepsilon_{G/S} - \varepsilon_{G/R}}{\Delta\theta}, \tag{4}$$

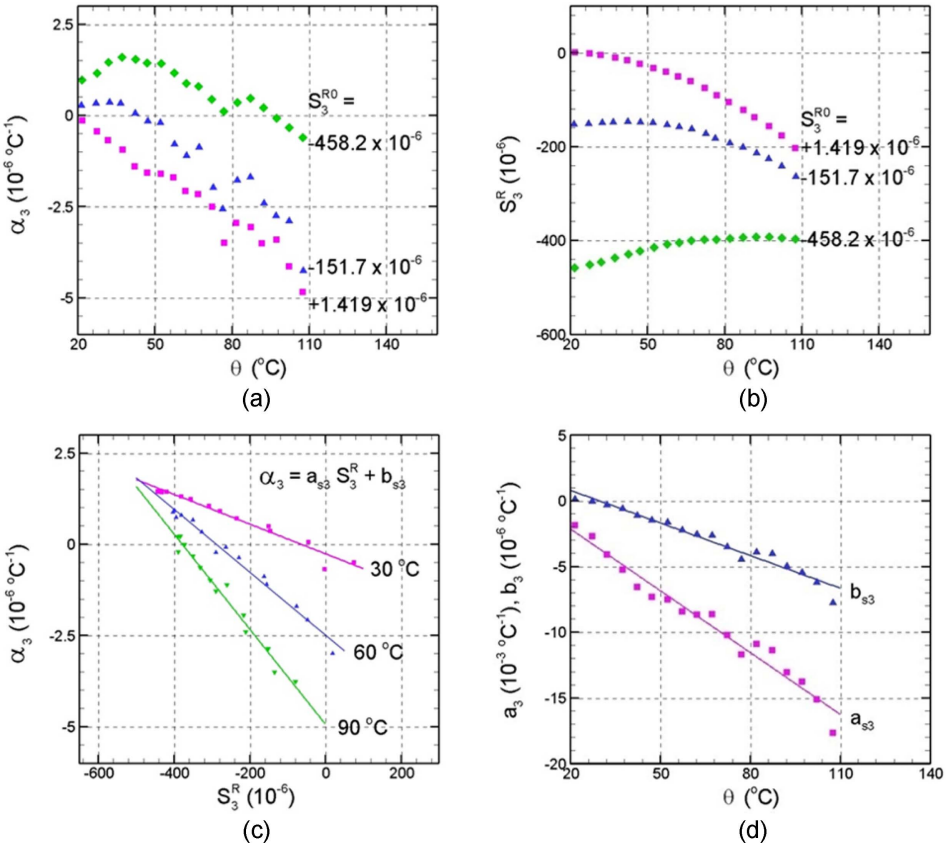

Fig. 3. Measured longitudinal thermal expansion coefficient α_3 and construction of empirical formula for α_3 during temperature rise at different values of reference remnant longitudinal strain S_3^{R0}, obtained by application of electric field at reference temperature of 20°C, (a) α_3 vs. θ at S_3^{R0} = +1.419 × 10^{-6}, –151.7 × 10^{-6} and –458.2 × 10^{-6}, (b) S_3^{R0} vs. θ, (c) α_3 vs. S_3^{R0} at θ = 30°C, 60°C and 90°C, (d) slopes α_{S3} and intercepts b_{S3} of the fitting straight lines in (c) vs. θ.

Here, α_S and α_R are the coefficients of thermal expansion for the ceramic and invar specimens, respectively.

The α_R value provided by the manufacturer was 0.75 × 10^{-6} °C^{-1}. $\varepsilon_{G/S}$ and $\varepsilon_{G/R}$ refer to the thermal powers measured using the strain gauges attached to the ceramic and invar specimens, respectively. 2-axis strain gauges were used, and the thermal power values in longitudinal and transverse directions were measured to calculate the longitudinal and transverse direction thermal expansion coefficients α_3 and α_1, respectively, using Eq. (4). $\Delta\theta$ is the temperature range of the thermal expansion coefficient measurement.

Figure 3(a) shows the variation in the longitudinal and transverse thermal expansion coefficients α_3 and α_1 for the ceramic specimen calculated using Eq. (4), plotted versus the temperature. The figure shows the variation in the longitudinal thermal expansion coefficient α_3 according to the temperature for the reference remnant strains +1.419 × 10^{-6}, –151.7 × 10^{-6}, and –458.2 × 10^{-6} among the total 14 reference remnant longitudinal strains S_3^{R0}. Integrating the thermal expansion coefficients of Fig. 3(a) results in the variation in remnant longitudinal strain over temperature for a constant reference longitudinal strain S_3^{R0} as shown in Fig. 3(b).

The integration is carried out as shown below for the remnant longitudinal and transverse strains S_3^R and S_1^R, respectively, using the Euler method.

$$(S_3^R)_{i+1} = \alpha_3(\theta_i)(\theta_{i+1} - \theta_i) + (S_3^R)_i,$$
$$(S_1^R)_{i+1} = \alpha_1(\theta_i)(\theta_{i+1} - \theta_i) + (S_1^R)_i, \quad (5)$$

Here, the Euler integration begins with the reference remnant longitudinal and transverse strains S_3^{R0} and S_1^{R0}, respectively, at the reference temperature θ = 20°C and is carried out until 110°C.

Figure 3(b) shows the calculated longitudinal and transverse remnant strains. In Fig. 3(b), the largest applied electric field at the reference temperature was S_3^{R0} = –458.2 × 10^{-6}. By the electric field at the reference temperature, the spontaneous polarizations of most domains in the initial polarization direction are switched to the perpendicular directions, and the longitudinal strain increased with temperature.

On the other hand, when S_3^{R0} = +1.419 × 10^{-6}, the magnitude of applied electric field was sufficiently small, so that the specimen could be considered to be in its initial poled state. Thus, when the temperature increased, the longitudinal strain decreased.

For the case of S_3^{R0} = –151.7 × 10^{-6} where a relatively

small electric field was applied, the longitudinal strain showed a complicated behavior: it slightly increased at low temperature, then decreased at high temperature. Using Fig. 3(b) again, the variation in longitudinal thermal expansion coefficient at constant temperatures over remnant longitudinal strain can be obtained.

Figure 3(c) shows the change in longitudinal thermal expansion coefficient for the constant temperatures of 30°C, 60°C, and 90°C, plotted versus the remnant strain. Interestingly, like the result in Fig. 2(b), the change in thermal expansion coefficient at constant temperature, when plotted versus the remnant state variables, can be fitted with a straight line. The slope a_{S3} and intercept b_{S3} values of the lines vary with temperature, and Fig. 3(d) shows the distribution over temperature. The slope and intercept data shown in Fig. 3(d) also show linear distributions, and the same method can also be used with the pyroelectric coefficient p_3 data in Fig. 2(c) to express the slope and intercept as linear equations. Equation (6) can be obtained when the linear equations in Fig. 3(d) are applied to the linear equations in Fig. 3(c).

$$\alpha_3 = (a_{S3\theta}\theta + a_{S30})S_3^R + (b_{S3\theta}\theta + b_{S30}) .$$
$$\alpha_1 = (a_{S1\theta}\theta + a_{S10})S_1^R + (b_{S1\theta}\theta + b_{S10}) . \quad (6)$$

Here, $a_{S3\theta}$ and $b_{S3\theta}$ are the slopes of the lines in Fig. 3(d). When the temperature is 0, the intercept values are a_{S30} and b_{S30}. The equations are similar to Eq. (3) for the pyroelectric coefficient, and the equation for the transverse direction strain S_1^R can be derived in the same manner. Using Eq. (6), the longitudinal (or transverse) thermal expansion coefficient α_3 (or α_1) can be obtained when the temperature θ and longitudinal (or transverse) remnant strain S_3^R (or S_1^R) are given.

3.3. Governing Differential Equations and Empirical Formula

The pyroelectric coefficient p_3 is the rate of change in the remnant polarization P_3^R with temperature, and it can be expressed as $p_3 = dP_3^R/d\theta$. Combining this equation with Eq. (3) gives the following differential equation.

$$\frac{dP_3^R}{d\theta} - (a_{P\theta}\theta + a_{P0})P_3^R = \pm (b_{P\theta}\theta + b_{P0}) , \quad (7)$$

In Eq. (7), the ± sign on the right side is related to the directions of the specimen polarization and the applied electric field at the reference temperature. The + sign corresponds to when the electric field is applied in the positive direction to the specimen poled in the negative direction, and the – sign corresponds to when the electric field is applied in the negative direction to the specimen poled in the positive direction. This is a natural result. Using the definitions of the longitudinal and transverse thermal expansion coefficients, the governing differential equations similar to Eq. (7) can be obtained for the longitudinal and transverse strains S_3^R and S_1^R, respectively. The following differential equation can be used to express the behavior of P_3^R, S_3^R, and S_1^R during temperature increase.

Table 1. Values of Coefficients in Differential Equations of Eqs. (8) and (9)

Dependent variable	Constants	Units of constants	Values of constants
P_3^R	$a_{p\theta}$	10^{-4}	–0.49856
	a_{p0}	10^{-4} °C	0.74173
	$b_{p\theta}$	10^{-4} Cm^{-2}	–0.0063591
	b_{p0}	10^{-4} Cm^{-2}°C	0.33110
S_3^R	$a_{S3\theta}$	10^{-3}	–0.15672
	a_{S30}	10^{-3} °C^{-1}	0.98349
	$b_{S3\theta}$	10^{-6}	–0.082690
	b_{S30}	10^{-6} °C^{-1}	2.4437
S_1^R	$a_{S1\theta}$	10^{-3}	–0.15694
	a_{S10}	10^{-4} °C^{-1}	0.85425
	$b_{S1\theta}$	10^{-6}	0.071871
	b_{S10}	10^{-6} °C^{-1}	1.0565

$$\frac{dY}{d\theta} - (a_\theta\theta + a_0)Y = b_\theta\theta + b_0 , \quad (8)$$

Here, the dependent variable Y can be P_3^R, S_3^R, or S_1^R. Likewise, a_θ is $a_{P\theta}$, $a_{S3\theta}$, or $a_{S1\theta}$, and a_0 is a_{P0}, a_{S30}, or a_{S10}, depending on the dependent variable. The values of a_θ and a_0 can be obtained from Figs. 2(c) and 3(d). The values are listed in Table 1. When the boundary conditions θ_1 and Y_1 are given, or in other words, when the value of the dependent variable Y_1 (P_{31}^R, S_{31}^R, or S_{11}^R) is given for a specific temperature θ_1, the variation in dependent variable Y with temperature can be obtained using Eq. (9).

$$Y(\theta) = \exp\left(\frac{a_\theta}{2}\theta^2 + a_0\theta\right) \left[Y_1 \exp\left(-\frac{a_\theta}{2}\theta_1^2 - a_0\theta_1\right) + \{I(\theta) - I(\theta_1)\}\right], \quad (9)$$

Here, $I(\theta)$ is expressed with Eq. (10) shown below.

$$I(\theta) = \int \exp\left(-\frac{a_\theta}{2}\theta^2 - a_0\theta\right)(b_\theta\theta + b_0)d\theta = \frac{1}{2(a_\theta)^{1.5}} \exp\left(-\frac{a_\theta}{2}\theta^2 - a_0\theta\right) \quad (10)$$
$$\left[-\sqrt{2\pi}\exp\left\{\frac{(a_\theta\theta + a_0)^2}{2a_\theta}\right\}(a_0b_\theta - a_\theta b_0)erf\left(\frac{a_\theta\theta + a_0}{\sqrt{2a_\theta}}\right) - 2\sqrt{a_\theta}b_\theta\right]$$

In Eq. (10), $erf(x)$ is the error function.

The temperature rise experiment was carried out using a new PZT specimen, and the analysis of the data revealed that the derived empirical equation (9) was the same as a previously derived equation. This shows that the process of establishing the governing differential equation can be generally applied to the nonlinear behavior of ferroelectric PZT

materials.[12]

3.4. Comparison of Calculated and Empirical Results

Figure 4 shows the changes in the remnant polarization P_3^R and the remnant longitudinal and transverse strains S_3^R and S_1^R, respectively. They were calculated using the empirical formula in Eq. (9) for the five reference remnant polarizations P_3^{R0} induced by the electric field at reference temperature.

Figure 4(a) shows the changes in remnant polarization. For the longitudinal and transverse strains, Fig. 4(b) shows the case when the reference remnant polarization was negative and Fig. 4(c) the case when the reference remnant polarization was positive. The experimentally measured values of P_3^R, S_3^R, and S_1^R are shown in the form of symbols in the figure. The five reference remnant polarizations shown in the figure are –0.256, –0.135, –0.018, +0.136, and +0.262 Cm^{-2}. Although the measurement temperature range was only from 20°C to 110°C, the variations in P_3^R, S_3^R, and S_1^R showed slightly nonlinear behavior in relation to the temperature.

However, to make an approximate calculation, it can be assumed that the remnant state variables vary at constant rates with the temperature. Comparisons of the calculated and measured values shows that they are in good agreement with each other for all states of reference remnant polarization. Thus, it is concluded that Eq. (9) can be used to predict the macroscopic changes in polarization and strains of ferroelectric specimens, when temperature is increased.

The rates in the changes in the measured values of P_3^R in Fig. 4 correspond to the pyroelectric coefficient, which were expressed with symbols in Fig. 5(a).

The predicted values of the pyroelectric coefficients can be obtained using Eq. (3) for given temperature and remnant polarization, and the calculated pyroelectric coefficient values are represented by solid curves in the same figure. It was observed that the calculated and experimental results were in relatively good agreement for the five reference remnant polarizations.

The thermal expansion coefficients obtained directly from experiments with the invar specimen are represented by solid curves in Figs. 5(b) and (c). In the same figures, the calculated values of thermal expansion coefficients from Eq. (6) are plotted by symbols. Like Figs. 4(b) and 4(c), Fig. 5(b) corresponds to the case where the reference remnant polarization was negative, and Fig. 5(c) corresponds to when it was positive. It was found that the calculated and experimental results were in relatively good agreement for all the reference remnant polarizations in the figure.

As mentioned in Fig. 4, if the changes in the remnant polarization and remnant strains are linear in relation to temperature for the relatively small temperature range from 20°C to 110°C, the pyroelectric and thermal expansion coefficients of Fig. 5 have to be assumed to be constant in the given temperature range. However, as can be observed in the figure, the thermal coefficients varies with the temperature, and therefore, the changes in thermal coefficients with temperature need to be included in the construction of an empirical modeling equation.

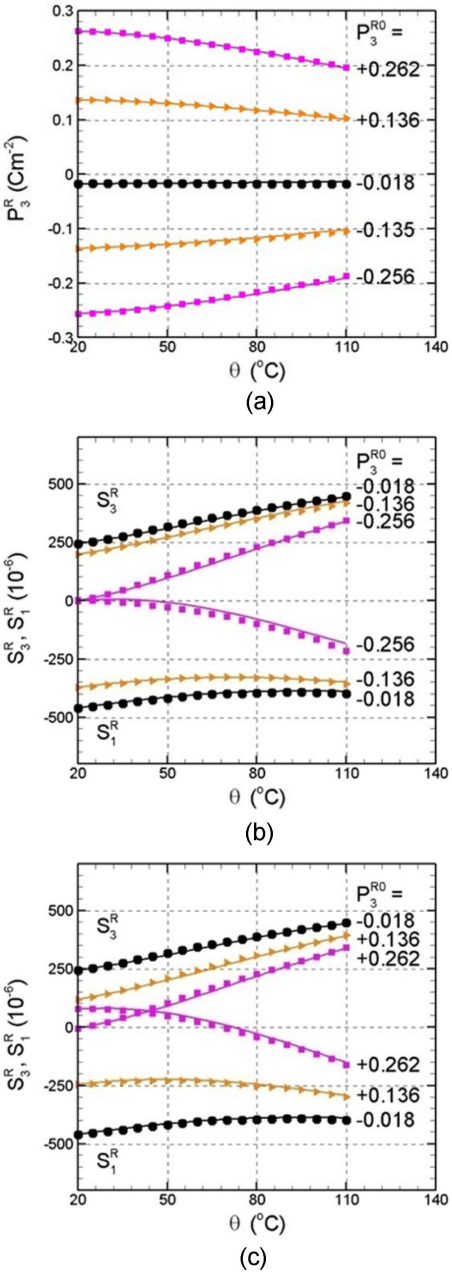

Fig. 4. Measured and predicted (a) remnant polarization P_3^R and (b, c) remnant longitudinal and transverse strains S_3^R and S_1^R. Measured data are represented by symbols, predictions are represented by line segments.

Lastly, the switching processes induced by an electric field were compared for different temperatures.

The research method used in this study was to investigate the nonlinear behavior of materials by observing changes in the remnant state variables, which represent the macroscopic behavior of the ferroelectric specimen. Then, the variations in the remnant polarization P_3^R and remnant strains

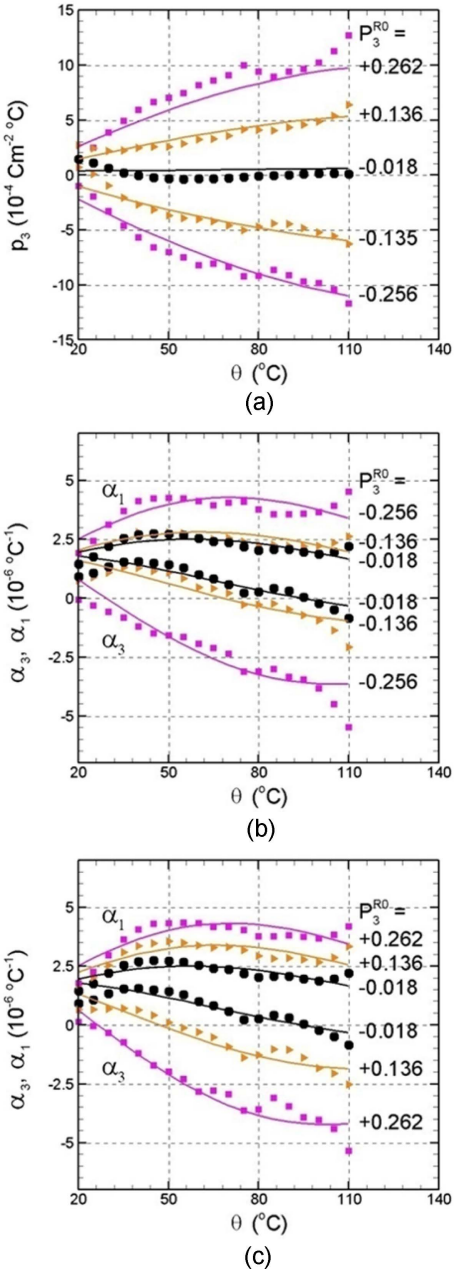

Fig. 5. Measured and predicted (a) pyroelectric coefficient p_3 and (b, c) longitudinal and transverse thermal expansion coefficients α_3 and α_1. Measured data are represented by symbols and predictions are represented by line segments.

S_3^R and S_1^R during the switching caused by the electric field, need to be plotted.

In this study, the changes in the state variables when the temperature of a ferroelectric specimen switched by an applied electric field at the reference temperature was increased, were investigated. Comparisons of the measured changes in the state variables during temperature rise and the predictions by the developed empirical formula showed a good agreement, as had been observed by experiment.[12)]

First, the state variables measured for temperatures of

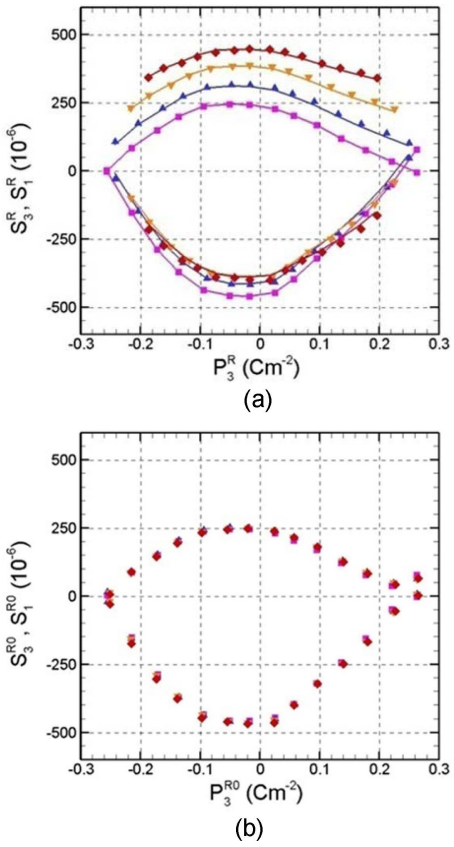

Fig. 6. Measured and predicted remnant state variables at four temperatures of 20°C, 50°C, 80°C and 110°C, represented by square, delta, gradient and diamond symbols, respectively. (a) S_3^R and S_1^R vs. P_3^R plots. Measured data are represented by symbols and predictions are represented by line segments. (b) S_3^{R0} and S_1^{R0} vs. P_3^{R0} plots. The data at 20°C are measured data and the reference remnant state variables corresponding to the measured data at 50°C, 80°C and 110°C are predicted data.

20°C, 50°C, 80°C, and 110°C are shown in Fig. 6(a), using square, triangle, inverted triangle, and diamond symbols, respectively. Also, the reference remnant variable values at 20°C were substituted into Eq. (9) to obtain the corresponding remnant variable values for 50°C, 80°C, and 110°C.

Figure 6(a) shows the calculated results in line form for each temperature case. In the figure, it can be observed that the prediction of the remnant strain variation with regard to the remnant polarization density is almost equivalent to the marked measurement results for the three temperature cases. By substituting the remnant state variable values measured for temperatures 50°C, 80°C, and 110°C in Eq. (9), the state variable values at reference temperature were obtained.

Figure 6(b) shows the reference remnant variables measured at 20°C, and the calculated reference remnant state variable values for three high temperatures. The reference remnant strain variations over reference remnant polarization were almost the same for all temperatures. This

implies that the relationships between the reference remnant state variables are the same when switching is caused by electric field.

In summary, it can be seen in Figs. 6(a) and (b) that the relationships between the macroscopic state variables are the same at different temperatures when switching is induced by an electric field. This means that the switching process by electric field is the same at different temperatures from the macroscopic point of view. If the microscopic domain structure corresponds to the macroscopic state variables on a one-to-one basis, this study shows that the process of change in the microscopic domain structure during switching by electric field is the same for different temperatures.

4. Conclusions

At the reference temperature, an electric field is applied in a direction opposite to polarization for a poled PZT ceramic specimen. After applying electric fields of 14 different magnitudes at the reference temperature, the temperatures of the ceramic specimen and invar specimen were increased from 20°C to 110°C. During the temperature increase, the remnant polarization and thermal expansion coefficient were measured. Using the measured values, differential equations governing the behavior of remnant polarization and remnant strains during the temperature rise were derived.

The empirical formula obtained from the governing differential equations was used to predict the changes in remnant polarization and remnant strains during temperature increase, and these values were then compared with the experimental results. The predicted and experimental results were in very good agreement for all the initial conditions. The predicted and experimental results for the pyroelectric and thermal expansion coefficients were also in good agreement with each other.

Finally, the switching processes due to an electric field at different temperatures were compared using the remnant state variables, and it was found that the switching processes by an electric field for the tested temperature range were equivalent, from a macroscopic state variable perspective.

The results of this study are similar to the results of a study conducted for a different PZT specimen, and they verify the validity of the derived empirical formula derived in this study.[12)]

Acknowledgments

This work was supported by the 2016 sabbatical year research grant of the University of Seoul.

REFERENCES

1. Q. D. Liu and J. E. Huber, "State Dependent Linear Moduli in Ferroelectrics," *Int. J. Solids Struct.,* **44** [17] 5635-50 (2007).
2. S. J. Kim, "A Constitutive Model for Thermo-Electromechanical Behavior of Ferroelectric Polycrystals near Room Temperature," *Int. J. Solids Struct.*, **48** [9] 1318-29 (2011).
3. H. Grunbichler, J. Kreith, R. Bermejo, P. Supancic, and R. Danzer, "Modelling of the Ferroic Material Behaviour of Piezoelectrics: Characterization of Temperature-Sensitive Functional Properties," *J. Eur. Ceram. Soc.,* **30** [2] 249-54 (2010).
4. H. Kungl and M. J. Hoffmann, "Temperature Dependence of Poling Strain and Strain under High Electric Fields in LaSr-doped Morphotropic PZT and its Relation to Changes in Structural Characteristics," *Acta Mater.,* **55** [17] 5780-91 (2007).
5. M. B. Rauls, W. Dong, J. E. Huber, and C. S. Lynch, "The Effect of Temperature on the Large Field Electromechanical Response of Relaxor Ferroelectric 8/65/35 PLZT," *Acta Mater.,* **59** [7] 2713-22 (2011).
6. M. S. Senousy, R. K. N. D. Rajapakse, and M. S. Gadala, "A Temperature-Dependent Two-Step Domain-Switching Model for Ferroelectric Materials," *Acta Mater.,* **57** [20] 6135-45 (2009).
7. D. W. Ji and S. J. Kim, "Measured Polarization Hysteresis and Predicted Reference Remnant Polarization and Strains of Ferroelectric Ceramics at Various Electric Field Loading Rates and Temperatures," *J. Korean Ceram. Soc.*, **51** [6] 591-97 (2014).
8. S. J. Kim and Y. S. Kim, "State Dependent Pyroelectric and Thermal Expansion Coefficients in a PZT Wafer," *Ceram. Int.*, **36** [7] 2189-96 (2010).
9. D. W. Ji and S. J. Kim, "Prediction of High Temperature Behavior of Ferroelectric Ceramics with State Dependent Thermal Moduli," *J. Ceram. Soc. Jpn.* **123** [1433] 52-8 (2015).
10. D. W. Ji and S. J. Kim, "State-Dependent Pyroelectric and Thermal Expansion Coefficients in a PZT Rectangular Parallelepiped after Compressive Loading and Unloading," *J. Mater. Sci.*, **49** [2] 766-75 (2014).
11. K. G. Webber, E. Aulbach, T. Key, M. Marsilius, T. Granzow, and J. Rödel, "Temperature-Dependent Ferroelastic Switching of Soft Lead Zirconate Titanate," *Acta Mater.,* **57** [15] 4614-23 (2009).
12. D. W. Ji and S. J. Kim, "Development and Application of an Empirical Formula for the High Temperature Behavior of Ferroelectric Ceramics Switched by Electric Field at Room Temperature," *AIP Adv.,* **7** 055316 (2017).
13. VISHAY Precision Group Technical Note, Measuremnet of Theral Expansion Coefficient Using Strain Gauges (Tech. Note TN-513-1, 2010; http://www.vishaypg.com/docs/11063/tn5131tn.pdf).